



Effects of global postural alignment on posture-stabilizing synergy and intermuscular coherence in bipedal standing

Stephen M. Glass¹ · Lane Wildman¹ · Cameron Brummitt¹ · Kevin Ratchford¹ · Grant M. Westbrook¹ · Adrian Aron¹

Received: 8 September 2021 / Accepted: 14 December 2021 / Published online: 22 January 2022
© The Author(s), under exclusive licence to Springer-Verlag GmbH Germany, part of Springer Nature 2021

Abstract

Clinicians frequently assess and intervene on postural alignment; however, notions of what constitutes good postural alignment are variable. Furthermore, the majority of current evidence appeals either to population norms or defines good postural alignment as the negation of what has been observed to correlate with pathology. The purpose of this study was to identify affirmative indicators of good postural alignment in reference to motor control theory. Electromyography (anterior leg, posterior leg, and trunk muscles) and motion capture data were acquired from 13 participants during 4 min bipedal standing trials in 4 conditions: control, – 10%, + 30%, and + 60% of subject-specific anterior limits of stability. Synergistic kinematic coordination was quantified via the uncontrolled manifold framework, and correlated neural drive was quantified in posture-relevant muscle groups (anterior, posterior, and trunk) via intermuscular coherence. Multilevel models assessed the effects of sagittal plane alignment on both outcomes. We observed a within-subjects fixed effect in which kinematic synergistic coordination decreased as subjects became more misaligned. We also observed within-subjects fixed effects for middle- and high-frequency intermuscular coherence in the posterior group (increased coherence with increased misalignment) and for trunk intermuscular coherence across all frequency bands (decreased coherence with increased misalignment). Our findings indicate that it may be possible to describe healthy postural alignment in light of referent control theory. Greater misalignment with respect to vertical is associated with compromises in synergistic control of posture and increased corticospinal drive to specific muscle groups. These results suggest that postural alignment may not simply be an empirical phenomenon.

Keywords Quiet standing · Intermuscular coherence · Synergy · Sagittal alignment

Introduction

The importance of global postural alignment has been recognized in clinical contexts for some time (Bullock-Saxton 1993; Schwab et al. 2006). While several accounts of postural alignment have been offered, these are most often empirical in nature (Ferreira et al. 2011; Hasegawa et al. 2017). As such, they appeal primarily to population norms when describing healthy postural alignment, or instead focus on defining what may be considered “bad” on the basis of correlation with adverse clinical outcomes. Thus, although the clinical application of postural alignment is

not unfounded, neither is it grounded in any sort of theory affirming notions of how postural alignment should—as opposed to should not—look. Indeed, some argue that a recent surge of interest in postural alignment has been accompanied by concomitant growth in a “posture industry” whose claims frequently lack hard evidence (Slater et al. 2019).

A lack of evidence notwithstanding many physical/sports medicine clinicians would likely agree that postural alignment should feature prominently as a component of patient care (Sahrmann 2002). However, lingering questions limit our ability to intervene effectively on postural alignment, especially at the individual level. The most fundamental of these questions concerns what defines “good” postural alignment. Subsequent questions might address whether “correct” posture varies within and/or between persons, how bad postures develop, and how posture can be improved. Regardless of whether one relies on a theoretical or empirical basis for defining good posture, the existing evidence is not sufficient

Communicated by Francesco Lacquaniti.

✉ Stephen M. Glass
smglass1@radford.edu

¹ Department of Physical Therapy, Radford University
Carilion, 101 S Elm Ave. #830, Roanoke, VA 24013, USA

to advocate strongly for one alignment pattern over another outside of avoiding patterns previously associated with negative outcomes. The evidence is even less sufficient to inform the assessment of alignment in a specific individual.

Within the past 20 or so years, movement scientists have arrived at valuable insights through the study of movement coordination and variability as adjuncts to research on aggregated movement behavior outcomes. Several analytical methods have been developed by which researchers can infer properties of the underlying movement system through observing the structure of its variability over time (Latash et al. 2002). Importantly, for cases in which an affirmative description of what is good is lacking—such as postural alignment—analyses of movement coordination and variability can provide an alternative basis for evaluation while simultaneously allowing us to draw on the authority of motor control theory (Latash et al. 2010).

The uncontrolled manifold framework (Hsu et al. 2007) (UCM) and intermuscular coherence (Laine and Valero-Cuevas 2017) (COH) are two such analyses well suited to the study of synergistic coordination in human movement. The first is a method of separating variability into goal-stabilizing vs. goal-destabilizing components within redundant degrees of freedom attending to functional tasks. The second quantifies common oscillatory input to neurally bound muscle pairs, thereby providing an indication of centrally prescribed synergistic grouping and—depending on the observed frequency distributions—a group's approximate neural origin (Laine and Valero-Cuevas 2017; Nandi et al. 2019). Both of these outcomes have been studied in the context of maintaining vertical posture (Watanabe et al. 2018; Yamagata et al. 2018), but to date we are unaware of any accounts specifically studying the relationships between alignment and strength of synergies as indicated by UCM and COH analyses. Mapping changes in postural alignment onto changes in synergistic motor behavior in this way could help move us toward affirmative, theoretically grounded indicators of healthy postural alignment.

The purposes of this study were to quantify the relationship between (1) postural alignment and synergistic joint angle variability, and (2) postural alignment and COH within relevant muscle synergies formed by anterior, posterior, and trunk muscle groups. For both aims, we modeled both within-subjects and between-subjects effects. Our findings are intended to support a larger line of inquiry aimed at identifying healthy and readily measurable patterns of postural alignment with particular emphasis on their relevance in applied settings. We hypothesized that within- and between-subjects synergistic joint angle variability would decrease as subjects become more misaligned with respect to the vertical. With respect to COH, we hypothesized that greater deviation from vertical sagittal alignment would coincide with a shift from low-frequency COH to middle- and

high-frequency COH for the posterior muscle group, similar to what has previously been demonstrated with anterior leaning tasks (Watanabe et al. 2018). Lacking evidence outside of the posterior muscle group, we extend this hypothesis to the trunk and anterior groups, as well.

Methods

The present research procedures were approved by the Radford University Institutional Review Board in accordance with The Declaration of Helsinki. All subjects provided written informed consent to participate in this study. All procedures were completed within the course of a single laboratory visit.

Participants

Seven females (24.57 ± 1.62 years, 164.36 ± 4.23 cm, 58.94 ± 12.34 kg) and six males (25.00 ± 2.28 years, 174.83 ± 8.82 cm, 81.25 ± 14.16 kg) participated in this study. Participation was limited to healthy, young adults without activity restrictions, history of pathologies affecting balance, or recent (<6 months) history of lower extremity or concussive injury.

Procedures

Following consent, retroreflective markers were affixed to the participant per the Vicon Plug-In-Gait marker set. Electromyography (EMG) sensors were placed bilaterally over the bellies of the rectus abdominis (RAB), anterior tibialis (ATIB), semitendinosus (SMT), medial gastrocnemius (GMED), rectus femoris (RFEM), and lumbar erector spinae (LES) muscles. Subjects then assumed a comfortable bipedal quiet standing posture with a self-selected foot position. This foot position was marked on the plate and used for all subsequent calibration and testing trials. From this position, subjects first performed two modified functional limits of stability (Lemay et al. 2014) (LOS) trials requiring them to lean as far as possible for 10 s in each of six directions—12, 2, 4, 6, 8, and 10 o'clock—without moving or lifting their feet. In contrast with more conventional methods of LOS testing, trials were performed without visual feedback and, to avoid constraining potentially informative joint variability, participants were not instructed to “hinge from the ankles” when leaning. During LOS trials, the approximate mean difference (Δ LOS) of the anteroposterior position of the PSIS markers at rest and during the 10 s period of leaning in the 12 o'clock direction was recorded. This difference was then used to calculate anteroposterior PSIS target positions corresponding to each lean level. For example,

the target PSIS position in the positive 60% lean trial was defined as [resting PSIS position + 0.6 × (ΔLOS)]. Similarly, the negative 10% target PSIS position was defined as [resting PSIS position − 0.1 × (ΔLOS)].

Next, participants completed a series of 4 barefoot quiet standing balance trials consisting of 1 or 2 trials in each of 4 anteroposterior lean conditions. Previously recorded ΔLOS values were used to define the following subject-specific lean targets: negative 10% (− 10), control (CON), positive 30% (+ 30), and positive 60% (+ 60). These levels represent target PSIS marker displacement from neutral as a percentage of ΔLOS. For example, the target PSIS position in the positive 60% lean trial was defined as (resting PSIS position + 0.6 × ΔLOS). Subjects were instructed to fix their gaze on a spot directly in front of them on the wall and maintain the lean target for the entire 4-min duration of a given lean trial. The motion capture operator provided the subject with one of three intermittent verbal feedback (D’Anna et al. 2015; Kilby et al. 2017) cues indicating the adjustment necessary to hit the target: (1) “forward”, (2) “back”, or (3) “good”. For all non-control conditions, these cues were provided every 30 s after trial initiation based on the real-time position data of the PSIS markers. In the CON condition, we were primarily interested in natural quiet standing behavior, which would not otherwise involve feedback. However, since all other conditions involved feedback, we provided feedback to a subset of participants in the CON condition to ensure that variability related to the mere presence of feedback would be reflected. Trials were presented in randomized order and subjects were permitted to sit between trials as needed.

Equipment

Marker trajectories were acquired at a frame rate of 100 Hz using an 8-camera VICON Bonita motion capture system with Nexus 2.11 (Vicon Motion Systems, Oxford, UK). EMG data were acquired at 1500 Hz using wireless

Noraxon DTS surface EMG (Noraxon USA Inc., Scottsdale, AZ) triggered through a Vicon MX Giganet.

Data processing

Marker trajectories were reconstructed in Nexus, exported, and used to compute sagittal plane joint angles for the ankle, knee, hip, thoracolumbar junction (TLJ), and neck. The same data were used to compute segment lengths for the tibia, thigh, abdomen, thorax, and head–neck as described in Table 1. Virtual markers were calculated as follows: segment center of mass (COM) locations were then estimated using Winter’s body segment parameters (Winter 2009) and the whole-body COM in the anteroposterior dimension was computed as a weighted sum of the individual segment COMs. Segment angles were then defined in the global coordinate system as the angle between the segment and the x-axis using the R function *atan2*. Finally, sagittal plane joint angles were defined as the differences between adjacent segment angles.

Global postural alignment was operationalized as the sum of the absolute values of segment angular deviation from vertical in the sagittal plane. Our use of segment angles as opposed to joint angles for this purpose ensures that each segment can affect the global alignment computation regardless of its relationship with adjoining segments.

All kinematic signals were low-pass filtered at 5 Hz (bi-directional fourth-order Butterworth filter) prior to further analysis.

Uncontrolled manifold and synergy index

Angular joint displacement over time was partitioned into goal equivalent (GEV) and non-goal equivalent (NGEV) variability based on its tendency to stabilize or deflect, respectively, the whole-body COM from its equilibrium point. Thus, in our analysis, the whole-body COM in the anteroposterior dimension represents the task variable, while the previously defined joint angles constitute the elemental variables. Postural sway reflects different sources of variability over multiple timescales (Yamagata et al. 2019), with

Table 1 Joint and segments’ definitions

	Segments	Inferior marker(s)	Superior marker(s)
Ankle	Shank, floor plane	Ankle joint center*	Lateral knee
Knee	Thigh, shank	Lateral knee	Hip joint center*
Hip	Lower trunk, thigh	Hip joint center*	Mid-thorax*
Mid-torso	Upper trunk, lower trunk	Mid-thorax*	Neck*
Neck	Head-neck, upper trunk	Neck*	Head*

Asterisks (*) indicate virtual marker calculations. Sagittal plane virtual marker coordinates were calculated from surface markers as follows: ankle joint center = average of medial and lateral malleoli; hip joint center = Harrington equations 5 and 6 (Harrington et al. 2007); mid-thorax = mean of T10 and Sternum (Xiphoid) markers; neck = mean of C7 and Clavicle (Manubrium) markers

the true equilibrium point of the COM likely migrating to some degree. To accommodate this behavior, we applied a separate low-pass filter to the whole-body COM with the intention of preserving salient COM displacement and used this new, slow-migrating COM (COM_S) to define our equilibrium point. The cut-off frequency used in this case—0.1 Hz—was selected based on the temporal characteristics of unintentional referent coordinate drifts (Yamagata et al. 2019). Note that, to separate GEV and NGEV around COM_S , we subtracted COM_S from the original whole-body COM to isolate the faster (COM_F) fluctuations that represent deviation from the migrating equilibrium point.

Prior to partitioning GEV and NGEV, the relationship between small changes in task and elemental variables must be specified by a matrix of partial derivatives (a Jacobian matrix). In our analysis, the Jacobian is defined as the transpose of the regression coefficients (de Freitas and Scholz 2010) predicting whole-body anteroposterior COM_F motion from sagittal plane joint angles

$$\Delta COM_F = \beta_1 \Delta \theta_{ANKLE} + \beta_2 \Delta \theta_{KNEE} + \beta_3 \Delta \theta_{HIP} + \beta_4 \Delta \theta_{TLJ} + \beta_5 \Delta \theta_{NECK}.$$

Variation within the null and orthogonal subspaces of this Jacobian represent, respectively, stabilizing vs. destabilizing angular joint motion. These subspace projections were computed for the deviation between instantaneous and mean joint angle configurations at each sample. Finally, joint angle variance within the null (GEV) and orthogonal (NGEV) subspaces over time was calculated and normalized by the dimension of the corresponding subspace ($GEV = 4$, $NGEV = 1$).

These UCM calculations were applied over each of 16 non-overlapping 15-s epochs. For each epoch, a synergy index expressing the relative proportion of total variance accounted for by stabilizing joint angle variability was defined as

$$\Delta_V = \frac{(GEV - NGEV)}{(GEV + NGEV)}.$$

A Fisher z-transformation was then applied to this synergy index (Solnik et al. 2013) to yield S_Z , which constituted the primary outcome to be used in statistical modeling of performance-stabilizing kinematic synergies

$$S_Z = 0.5 \times \log \left(\frac{|\text{Min } \Delta_V| + \Delta_V}{\text{Max } \Delta_V - \Delta_V} \right) - 0.5 \times \log \left(\frac{|\text{Min } \Delta_V|}{\text{Max } \Delta_V} \right).$$

EMG amplitude and frequency analysis

As with kinematic data, raw EMG recordings were segmented into 15-s epochs ($n = 16$) per trial prior to further

processing. EMG signals were visually inspected for artifacts. Muscle-epochs (i.e., epochs per muscle) containing visible artifacts were excluded from analysis.

Raw EMG data were bandpass filtered between 20 and 500 Hz (bi-directional fourth-order Butterworth) and rectified. Muscle activation levels (MALs) were then computed as the mean amplitude for each epoch. For each subject * muscle * epoch, signals were normalized by the corresponding amplitude from the no-lean (CON) condition. Therefore, MALs express amplitude as a multiple of the baseline value (Nandi et al. 2019). MALs are presented for descriptive purposes, but did not feature in our predictive models.

For coherence analysis, raw EMG were high-pass filtered at a cut-off frequency of 250 Hz (Laine and Valero-Cuevas 2017) (bi-directional fourth-order Butterworth) and rectified. Auto- and cross-spectra were estimated for each signal from non-overlapping Hanning windows of 1500 samples of the filtered and rectified EMG. Single pair coherence was calculated in the 0–56 Hz range for ipsilateral muscle pairs contributing to groups representing three synergies: (1) anterior (ATIB, RFEM, RAB), (2) posterior (GMED, SMT, LES), and (3) trunk (LES, RAB), similar to what has been described in the previous reports (Krishnamoorthy et al. 2003; Danna-Dos-Santos et al. 2014). Coherence values were computed as the magnitude squared cross-spectrum divided by the product of the auto-spectra

$$|R_{xy}(\lambda)|^2 = \frac{|f_{xy}(\lambda)|^2}{|f_{xx}(\lambda)f_{yy}(\lambda)|}.$$

Pooled coherences for each mode were then computed as

$$\frac{|\sum_{i=1}^k f_{xy}(\lambda)Li|^2}{(\sum_{i=1}^k f_{xx}(\lambda)Li)(\sum_{i=1}^k f_{yy}(\lambda)Li)},$$

where k indicates the number of constituent single pair coherence values, each calculated over L windows.

Finally, pooled coherence profiles from were integrated over three frequency ranges. These ranges were chosen to reflect the methods reported in Nandi et al. (2019) albeit with a greater ceiling for the highest range (Poston et al. 2010). Specifically, we integrated coherence estimates from 0 to 5 Hz, 6 to 15 Hz, and 16 to 56 Hz. Although the precise sources of coherence signatures in these frequency bands are not known, the first band is interpreted to reflect subcortical drive and the latter two are interpreted to reflect corticospinal drive (Nandi et al. 2019).

Statistical analysis

Aggregated data were screened for multivariate outliers based on Mahalanobis distance. Observations whose Mahalanobis

distance exceeded the critical Chi-square value ($\alpha = 0.01$) were excluded from analysis.

Multilevel models

We used the “Random Effects Within Between” (REWB) (Bell et al. 2019) model to study the effects of postural alignment on S_z and COH. The REWB model accounts for fixed effects both within and between subjects, as well as a subject-specific random effect. This latter effect allows the within-subject fixed effect to vary across subjects (Bell et al. 2019). The model was specified as follows:

$$\text{lmer}(\text{Outcome} \sim 1 + \Sigma\Theta_{PS} + \Sigma\Theta_{CM} + (\Sigma\Theta_{PS} | \text{subj})),$$

where “PS” designates a person-SD-centered (Wang et al. 2019) predictors and “CM” designates the mean of the cluster (i.e., person) within which measures are repeated. Conditional and marginal R^2 were approximated as reported in Nakagawa et al. (2013). Data reduction and statistical analyses were performed in R (The R Foundation, Vienna, Austria) using custom scripts and additional functions from the nlme, lme4, effects, and ggplot2 packages.

Results

Four participants completed two trials in every balance condition. One participant repeated 3 conditions, and another repeated 2. The remaining participants completed a single trial in each condition. Data for two participants (s07, s09) were discarded listwise due to excessive marker dropout, as were two trials for participant s06. (At least 1 trial from each condition was retained for s06.) We also note that technical difficulties required that acquisitions for the first two subjects be manually synchronized.

Out of 1,104 epochs of kinematic data, 5 (0.45%) were identified as multivariate outliers and discarded. After removing EMG data for which no matching kinematic data were retained, an additional 115 muscle-epochs (0.75%) were excluded after visual inspection. Finally, 27 cases in the aggregated EMG dataset (2.52%) were identified as multivariate outliers and discarded prior to modeling.

Means and standard deviations are reported in Tables 2 (S_z) and 3 (COH). Mean MALs by condition are depicted in Fig. 1 (left and right muscles are averaged), while Fig. 2 shows mean sagittal plane joint positions in each lean condition. Figures 3

and 4 show scatterplots of S_z (Fig. 3) and COH (Fig. 4) against sagittal plane alignment.

Alignment and synergistic joint angle variability

In the S_z model, the standard deviation of the random-effects intercept and slope estimates for $\Sigma\Theta_{PS}$ were 0.1498 and 0.0485, respectively. The correlation between these random slope and intercept estimates was 0.889. Marginal R^2 , indicating explained variance attributable to fixed effects, was 0.03. The conditional R^2 , indicating total variance explained, was 0.11. A significant fixed effect of within-subject—but not between-subject—alignment ($\Sigma\Theta_{PS}$) on S_z was observed (Table 2). Within-subject S_z tended to decrease as deviation from vertical alignment increased.

Alignment and intermuscular coherence

The effect of alignment on COH varied by muscle group (Table 3, Fig. 4). Neither within-subjects nor between-subjects effects of alignment on coherence in the anterior muscle group were significant in any frequency band. For the posterior muscle group, we observed a significant fixed effect of within-subjects alignment on COH in the middle- and high-frequency bands, with COH increasing as individuals deviated further from the vertical. Finally, we observed significant fixed effects of within-subjects alignment on COH in the trunk muscle group in all frequency bands. Unlike the effects observed for the posterior group, COH in the trunk group decreased as individuals deviated from vertical alignment.

Marginal R^2 values (Table 4) were comparable in magnitude to that observed for S_z . Conditional R^2 values ranged from moderate (~0.12) to extremely high (~0.92), possibly suggesting that random slope and intercept effects add substantial explanatory value for these particular models. The highest conditional R^2 values were observed in the low-frequency band and/or trunk muscle group analyses.

Discussion

This study quantified relationships between (1) postural alignment and S_z , and (2) postural alignment and COH in synergistic muscle groups relevant to the maintenance of upright stance. Our motivation for undertaking this study was to begin

Table 2 Fixed-effects summary for S_z model

Int			$\Sigma\Theta_{PS}$			$\Sigma\Theta_{CM}$		
Coef	<i>t</i>	<i>P</i>	Coef	<i>t</i>	<i>P</i>	Coef	<i>t</i>	<i>P</i>
1.2725	6.1795	0.0000	- 0.0807	- 3.6822	0.0002	- 0.0081	- 1.4889	0.1646

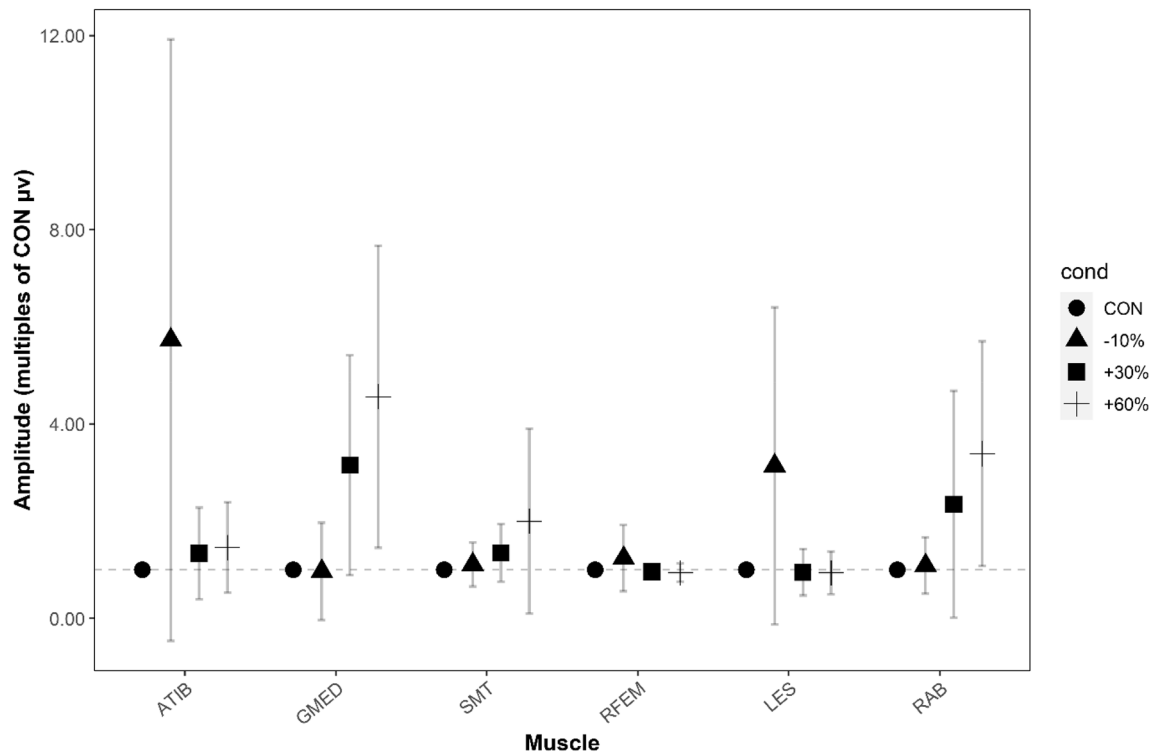


Fig. 1 Muscle activation levels (average of left/right muscle pairs) in each lean condition. Each mean represents that muscle's activation level in multiples of its baseline (CON condition) activation level.

Error bars represent standard deviation. *ATIB* anterior tibialis, *GMED* medial gastrocnemius, *SMT* semitendinosus, *RFEM* rectus femoris, *LES* lumbar erector spinae, *RAB* rectus abdominis

a process of gathering theory-based evidence to support clinical assessment of, and intervention on, posture in individual cases. We observed behavioral signatures of motor abundance as postural alignment varied both spontaneously and through subtle experimental tasks. Our results suggest that sagittal plane alignment is associated with S_z and COH, which in turn may indicate that there are theoretical reasons to prefer one postural configuration over another. We note here, however, that this study was not designed to identify specifically what those postures are or for whom they are to be preferred; rather, we interpret the present findings as adding to the evidence that alignment is not merely an empirical phenomenon. We discuss the S_z results first.

Alignment and kinematic synergy

In the context of the principle of motor abundance (Latash et al. 2010), synergies can be thought of as the hierarchical organization of numerous degrees of freedom into functional elements that coordinate to achieve a task-specific performance goal. Several previous studies have demonstrated synergistic control of the COM or similar variables in static standing tasks (Hsu et al. 2007; Park et al. 2016; Yamagata et al. 2018), although not necessarily with explicit relation to vertical alignment. As has been observed in prior work,

our study found that joints coordinated their angular motion to stabilize the COM (i.e., $GEV > NGEV$), in this case with respect to its migrating target. Such findings are certainly interesting of their own accord, but in the present context, we emphasize the broader theoretical implications. The lack of a postural template by which we can define good vs. bad alignment leaves us in the position of having to infer what “good” is in light of theoretical considerations. The synergy index S_z as computed via the UCM approach, in addition to providing an intuitive indicator of performance-stabilizing coordination, is consistent with the theory of motor control via specification of referent coordinates, as well as the associated growing body of evidence (Zhang et al. 2018).

Whereas previous studies on performance-stabilizing synergies in postural tasks focus largely on the control parameters involved in maintenance of upright stance, our eventual aim with the current line of inquiry is to identify what that stance looks like on average. In this regard, our work can be seen as an attempt to combine theory-rich accounts of postural control with empirical accounts of postural alignment, the latter being more often represented in the ergonomics and surgery literature (Hasegawa et al. 2017). The methods we used do not permit direct numerical comparison with normative alignment profiles offered in the previous works; however, we show qualitatively similar findings with respect

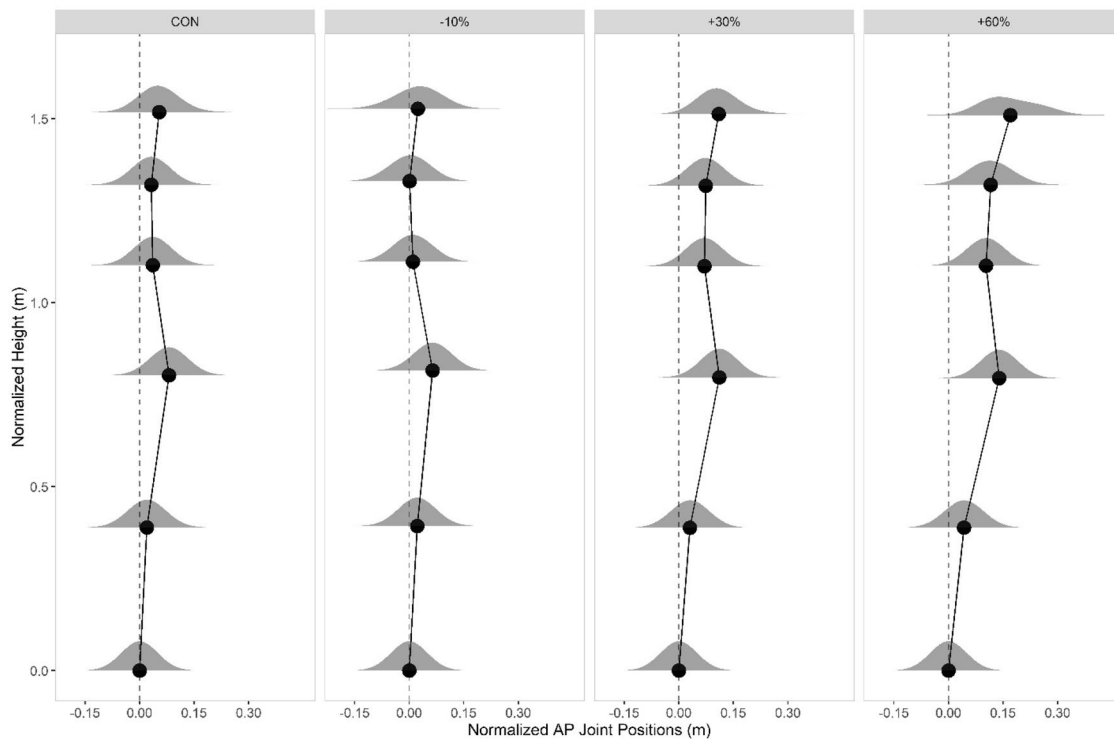


Fig. 2 Means across all subjects of sagittal plane joint positions computed from marker trajectories. Each joint is depicted at the center of a corresponding density plot representing its variability. From inferior

to superior, means and distributions are shown for the ankle, knee, hip, thoracolumbar junction, neck, and center of the head. For plotting purposes, height was normalized across subjects

to relationships between major load-bearing joints in the sagittal plane (Hasegawa et al. 2017; Yoshihara et al. 2018). Our concurrent observation that synergistic COM control tended to decrease as individuals in our sample became more misaligned adds an important behavioral indicator to a body of literature that traditionally appeals to quality of life or longitudinal risk outcomes. With this addition, we attempt to offer a pathway toward optimization of postural alignment as opposed to evaluating posture by reference to its association with negative outcomes (Kamitani et al. 2013; Yoshihara et al. 2018).

Intermuscular coherence

Frequency domain correlations, i.e., COH, between effector muscle pairs are another outcome hypothesized to reflect synergistic organization of elemental motor control variables (Danna-Dos-Santos et al. 2014). Before proceeding, it bears mentioning that “synergy” may imply any of several distinct meanings. In the context of muscle coordination, the term “synergy” sometimes refers to a group of muscles that coactivate incidentally—for example, when concurrent subcomponents of a complex task produce temporally correlated bursts of EMG amplitude. Such correlation may reflect synergistic coordination in the sense that all subcomponents

contribute to the task, but does not by itself indicate a central strategy of functional grouping to reduce the dimensionality of the control space. By contrast, intermuscular coherence signifies prescriptive, synergistic neural binding in support of functional tasks (Laine and Valero-Cuevas 2017; Nandi et al. 2019). Furthermore, the frequency characteristics of coherent muscle pairs provide some indication of the neural sources of their activation drive, although precise origins mostly remain unknown. Whatever the extent and origin of prescriptive neural binding, it should also be noted that COH as we present it here does not explicitly quantify how muscles contribute to goal equivalent vs. non-goal equivalent variability in task performance as was the case in our kinematic analyses.

Our experimental procedures purposely called for intermittent (as opposed to continuous (Watanabe et al. 2018)) feedback regarding a participant’s lean position with respect to the target. The purpose was to preserve as much as possible the spontaneous, unconstrained nature of quiet standing while also maintaining some degree of consistency in lean magnitudes. Notwithstanding, we hypothesized based on previous findings (Watanabe et al. 2018) that greater sagittal plane misalignment would be accompanied by a decrease in low-frequency COH, as well as increases in middle- and high-frequency COH, possibly reflecting a shift toward

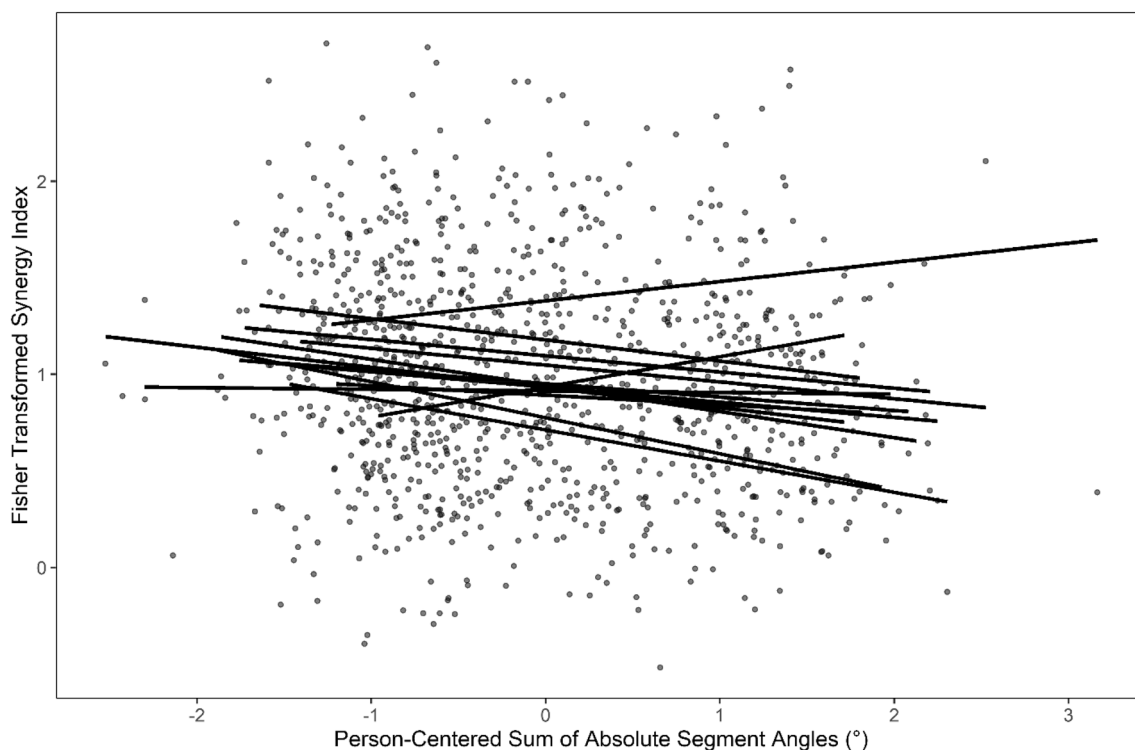


Fig. 3 Synergy index (S_z) plotted against sagittal plane deviation from perfect vertical alignment. The alignment variable is person-centered and person-standardized, and a linear regression is fitted

for each subject, to aid in the visualization of within-subject effects. Greater x-axis values indicated greater misalignment in the sagittal plane

higher level CNS involvement (Nandi et al. 2019). Instead, our results varied by muscle group, which could suggest more nuanced or task-dependent COH effects.

More specifically, as participants became deviated further from vertical alignment, we observed an increase in middle- and high-frequency COH for the posterior muscle group and a decrease in COH for all frequency bands in the trunk muscle group. A potential explanation based on the nature of the task could be that the posterior group was primarily responsible for active stabilization of the torques generated by what was mostly anterior misalignment (Mullick et al. 2018). Indeed, the observed muscle activation levels could support such a conclusion. The COH changes observed in the posterior group are consistent with increased corticospinal drive, but show no evidence of decreasing subcortical drive as was hypothesized. Thus, rather than low-frequency COH being displaced, it appears that the misalignment created by our leaning task added other sources of neural drive to the posterior muscle group. Previous reports in which subcortical drive was observed to decrease may be specific to bilateral muscle pairs and/or the use of continuous visual feedback (Watanabe et al. 2018), neither of which were of interest in the current study.

Our COH observations raise two questions: (1) what was the purpose of the increased corticospinal drive in the posterior muscle group, and (2) why were similar

changes in corticospinal drive not observed in the anterior and trunk muscle groups? Corticospinal pathways play an important role in controlling the threshold at which stretch reflexes are activated (Mullick et al. 2018), which is close to (if not equivalent to) the referent coordinate underlying referent control of posture. Among other performance variables, referent control may regulate both body configuration and body orientation. Body configuration concerns the relative positioning of body segments, whereas body orientation gives additional consideration to the direction of gravity (Mullick et al. 2018). Increased corticospinal drive with forward leaning may suggest that the posterior group became increasingly involved in the control of body configuration specifically (Mullick et al. 2018). That corticospinal drive in the anterior or trunk muscle groups was not observed to increase with misalignment is most easily explained by the nature of the task. Namely, static forward leaning may not call for such modulation of the stretch reflex outside of the posterior muscle group. The nervous system might use the effect of gravity, deeper (i.e., unmeasured) muscles, or passive mechanical joint properties in lieu of increasing corticospinal drive to other muscle groups (Zhang et al. 2018). Thus, the effects we would otherwise expect based on intention or task difficulty were limited to groups required for execution of the task. The

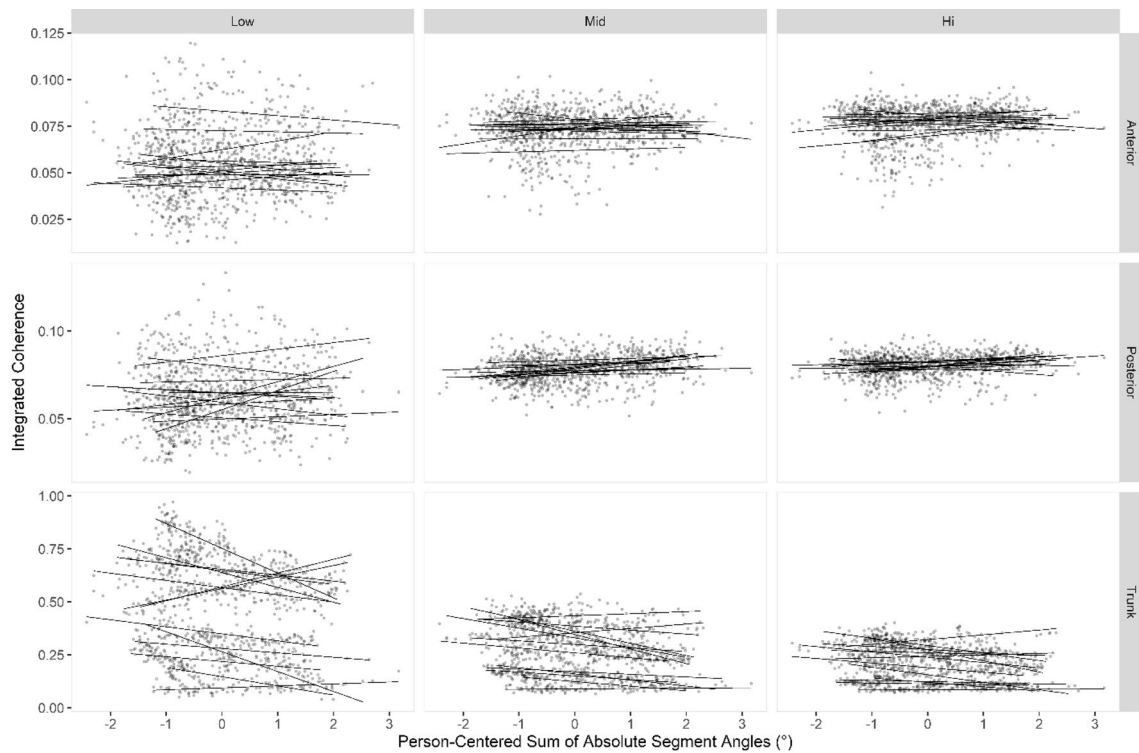


Fig. 4 Pooled, integrated COH for all pairs contributing to each of three muscle modes (anterior chain, posterior chain, and trunk) in each of three frequency bands (low=0–5 Hz, mid=6–22 Hz, and hi=23–56 Hz). The x-axis shows sagittal plane deviation from per-

fect vertical alignment as in Fig. 3. (Note, the scaling and range of the y-axis changes for the different muscle modes.) Lines represent subject-specific linear regressions fit to the data depicted in each subplot

Table 3 Fixed-effects summaries for COH models

Band	Int			$\sum\Theta_{PS}$			$\sum\Theta_{CM}$		
	Coef	<i>t</i>	<i>P</i>	Coef	<i>t</i>	<i>P</i>	Coef	<i>t</i>	<i>P</i>
Anterior									
Low	0.0674	4.0015	0.0001	0.0001	0.1972	0.8437	-0.0003	-0.7204	0.4863
Mid	0.0796	12.4111	0.0000	0.0003	0.7093	0.4783	-0.0002	-0.9501	0.3624
Hi	0.0817	17.1398	0.0000	0.0008	1.7099	0.0876	-0.0001	-0.9661	0.3548
Posterior									
Low	0.0697	4.3740	0.0000	0.0014	1.1416	0.2539	-0.0002	-0.3817	0.7100
Mid	0.0754	20.6668	0.0000	0.0018	5.0265	0.0000	0.0001	0.8619	0.4071
Hi	0.0793	31.6796	0.0000	0.0010	2.5149	0.0121	0.0000	0.4772	0.6426
Trunk									
Low	0.5120	1.5052	0.1326	-0.0283	-2.0825	0.0375	-0.0019	-0.2091	0.8382
Mid	0.3148	1.8081	0.0709	-0.0215	-3.2010	0.0014	-0.0013	-0.2829	0.7825
Hi	0.2362	1.9326	0.0536	-0.0146	-2.7223	0.0066	-0.0008	-0.2425	0.8129

specific COH responses of the trunk and anterior muscle groups may simply be a reflection of which sources of neural drive could be offloaded in which muscle groups.

Limitations

Several limitations of the current study should be noted. First, it is important to emphasize that 1) the within-subjects fixed effect appears to be more salient than the between-subjects fixed effect and, 2) we cannot say how

Table 4 Model fit and random-effects variability for COH analyses

Band	Int (SD)	$\sum\Theta_{ps}$	RE Corr	Marg. R^2	Cond. R^2
Anterior					
Low	0.0105	0.0018	− 0.1850	0.0173	0.3349
Mid	0.0039	0.0014	− 0.0530	0.0168	0.1898
Hi	0.0033	0.0015	− 0.5790	0.0187	0.1764
Posterior					
Low	0.0098	0.0040	− 0.1070	0.0089	0.3420
Mid	0.0021	0.0010	− 0.0750	0.0624	0.1550
Hi	0.0014	0.0013	− 0.0450	0.0290	0.1225
Trunk					
Low	0.2134	0.0484	− 0.1170	0.0191	0.9249
Mid	0.1094	0.0237	− 0.1310	0.0379	0.8802
Hi	0.0764	0.0190	− 0.0820	0.0343	0.8866

meaningful the observed behavioral changes are as a surrogate for the quality of postural alignment. Accordingly, our conclusions are primarily limited to the directionality of the observed effects rather than their utility in ascribing value to different patterns of alignment in a specific individual.

Additionally, our scalar alignment variable ($\sum\Theta$) does not fully describe changes in body configuration and assumes that the measured behavioral responses change linearly as segment angles deviate from vertical. While each of these assumptions is likely wrong, describing specifically where they fail will require additional study.

Third, the use of surface EMG to quantify COH is naturally limited to superficial muscles. Although it was not possible to quantify their activity in our lab, we must consider the possibilities that deeper muscles are more relevant to synergistic regulation of body orientation/configuration and that muscle synergies span a more comprehensive set of muscle pairs.

Further regarding our EMG methods, our functional muscle groups were defined on the basis of previous work in which muscle synergies were identified by correlations in EMG amplitude (Krishnamoorthy et al. 2003). As such methods cannot confirm prescriptive neural binding, it is possible that other muscle groups would better quantify the extent of centrally driven muscular synergy.

Finally, we cannot say based on our findings whether alignment had a causative role in producing the observed responses. Alignment may be a secondary feature of some other physiological process. Even so, we are ultimately interested in the viability of alignment as a clinical target, which does not necessarily require that it be the most proximate cause of a criterion response.

Conclusion

In conclusion, this study quantified behavioral indicators of synergistic motor coordination (kinematic and muscular) as a function of postural alignment. Our observations support the notion that it may be possible to evaluate alignment on theoretical grounds—specifically on the basis of referent control—with cumulative segment angulation in the sagittal plane tending to associate with compromised COM-stabilizing coordination and increased corticospinal drive in muscles contributing to the posterior muscle synergy.

Author contributions Conceptualization [all authors]; methodology [SMG]; formal analysis [SMG]; investigation [LW, CB, KR, GW]; funding acquisition [SMG, AA]; project administration [LW, CB, KR, GW]; writing—original draft [SMG]; writing—review and editing [all authors].

Funding This work was supported by an internal grant from the Radford University Office of Sponsored Programs and Grants Management awarded to SMG and AA.

Availability of data and materials Data and materials are available from the corresponding author upon reasonable request.

Code availability Software is available from the corresponding author upon reasonable request.

Declarations

Conflict of interest The authors have no conflicts of interest to report.

Ethical approval Study methods were approved by the Radford University Institutional Review Board in accordance with the Declaration of Helsinki.

Consent to participate All subjects provided written informed consent prior to participating in the study.

References

- Bell A, Fairbrother M, Jones K (2019) Fixed and random effects models: making an informed choice. *Qual Quant* 53:1051–1074
- Bullock-Saxton J (1993) Postural alignment in standing: a repeatability study. *Aust J Physiother* 39:25–29. [https://doi.org/10.1016/S0004-9514\(14\)60466-9](https://doi.org/10.1016/S0004-9514(14)60466-9)
- D’Anna C, Schmid M, Bibbo D, Bertollo M, Comani S, Conforto S (2015) The effect of continuous and discretized presentations of concurrent augmented visual biofeedback on postural control in quiet stance. *PLoS ONE* 10:e0132711. <https://doi.org/10.1371/journal.pone.0132711>
- Danna-Dos-Santos A, Boonstra TW, Degani AM, Cardoso VS, Magalhaes AT, Mochizuki L, Leonard CT (2014) Multi-muscle control during bipedal stance: an EMG–EMG analysis approach. *Exp Brain Res* 232:75–87

- de Freitas SM, Scholz JP (2010) A comparison of methods for identifying the Jacobian for uncontrolled manifold variance analysis. *J Biomech* 43:775–777. <https://doi.org/10.1016/j.jbiomech.2009.10.033>
- Ferreira EA, Duarte M, Maldonado EP, Bersanetti AA, Marques AP (2011) Quantitative assessment of postural alignment in young adults based on photographs of anterior, posterior, and lateral views. *J Manip Physiol Ther* 34:371–380. <https://doi.org/10.1016/j.jmpt.2011.05.018>
- Harrington ME, Zavatsky AB, Lawson SEM, Yuan Z, Theologis TN (2007) Prediction of the hip joint centre in adults, children, and patients with cerebral palsy based on magnetic resonance imaging. *J Biomech* 40:595–602. <https://doi.org/10.1016/j.jbiomech.2006.02.003>
- Hasegawa K, Okamoto M, Hatsushikano S, Shimoda H, Ono M, Homma T, Watanabe K (2017) Standing sagittal alignment of the whole axial skeleton with reference to the gravity line in humans. *J Anat* 230:619–630. <https://doi.org/10.1111/joa.12586>
- Hsu WL, Scholz JP, Schoner G, Jeka JJ, Kiemel T (2007) Control and estimation of posture during quiet stance depends on multijoint coordination. *J Neurophysiol* 97:3024–3035. <https://doi.org/10.1152/jn.01142.2006>
- Kamitani K, Michikawa T, Iwasawa S, Eto N, Tanaka T, Takebayashi T, Nishiwaki Y (2013) Spinal posture in the sagittal plane is associated with future dependence in activities of daily living: a community-based cohort study of older adults in Japan. *J Gerontol A Biol Sci Med Sci* 68:869–875
- Kilby MC, Molenaar PC, Slobounov SM, Newell KM (2017) Real-time visual feedback of COM and COP motion properties differentially modifies postural control structures. *Exp Brain Res* 235:109–120. <https://doi.org/10.1007/s00221-016-4769-3>
- Krishnamoorthy V, Goodman S, Zatsiorsky V, Latash ML (2003) Muscle synergies during shifts of the center of pressure by standing persons: identification of muscle modes. *Biol Cybern* 89:152–161. <https://doi.org/10.1007/s00422-003-0419-5>
- Laine CM, Valero-Cuevas FJ (2017) Intermuscular coherence reflects functional coordination. *J Neurophysiol* 118:1775–1783. <https://doi.org/10.1152/jn.00204.2017>
- Latash ML, Scholz JP, Schoner G (2002) Motor control strategies revealed in the structure of motor variability. *Exerc Sport Sci Rev* 30:26–31. <https://doi.org/10.1097/00003677-200201000-00006>
- Latash ML, Levin MF, Scholz JP, Schöner G (2010) Motor control theories and their applications. *Medicina* 46:382
- Lemay JF, Gagnon DH, Nadeau S, Grangeon M, Gauthier C, Duclos C (2014) Center-of-pressure total trajectory length is a complementary measure to maximum excursion to better differentiate multidirectional standing limits of stability between individuals with incomplete spinal cord injury and able-bodied individuals. *J Neuroeng Rehabil* 11:8. <https://doi.org/10.1186/1743-0003-11-8>
- Mullick AA, Turpin NA, Hsu SC, Subramanian SK, Feldman AG, Levin MF (2018) Referent control of the orientation of posture and movement in the gravitational field. *Exp Brain Res* 236:381–398. <https://doi.org/10.1007/s00221-017-5133-y>
- Nakagawa S, Schielzeth H, O'Hara RB (2013) A general and simple method for obtaining R² from generalized linear mixed-effects models. *Methods Ecol Evol* 4:133–142. <https://doi.org/10.1111/j.2041-210x.2012.00261.x>
- Nandi T, Hortobagyi T, van Keeken HG, Salem GJ, Lamoth CJC (2019) Standing task difficulty related increase in agonist-agonist and agonist-antagonist common inputs are driven by corticospinal and subcortical inputs respectively. *Sci Rep* 9:2439. <https://doi.org/10.1038/s41598-019-39197-z>
- Park E, Reimann H, Schoner G (2016) Coordination of muscle torques stabilizes upright standing posture: an UCM analysis. *Exp Brain Res* 234:1757–1767. <https://doi.org/10.1007/s00221-016-4576-x>
- Poston B, Danna-Dos Santos A, Jesunathadas M, Hamm TM, Santello M (2010) Force-independent distribution of correlated neural inputs to hand muscles during three-digit grasping. *J Neurophysiol* 104:1141–1154. <https://doi.org/10.1152/jn.00185.2010>
- Sahrmann SA (2002) Does postural assessment contribute to patient care? *J Orthop Sports Phys Ther* 32:4
- Schwab F, Lafage V, Boyce R, Skalli W, Farcy JP (2006) Gravity line analysis in adult volunteers: age-related correlation with spinal parameters, pelvic parameters, and foot position. *Spine (Phila Pa 1976)* 31:E959–967. <https://doi.org/10.1097/01.brs.0000248126.96737.0f>
- Slater D, Korakakis V, O'Sullivan P, Nolan D, O'Sullivan K (2019) Sit up straight: time to re-evaluate. *J Orthop Sports Phys Ther* 49:562–564. <https://doi.org/10.2519/jospt.2019.0610>
- Solnik S, Pazin N, Coelho CJ, Rosenbaum DA, Scholz JP, Zatsiorsky VM, Latash ML (2013) End-state comfort and joint configuration variance during reaching. *Exp Brain Res* 225:431–442. <https://doi.org/10.1007/s00221-012-3383-2>
- Wang L, Zhang Q, Maxwell SE, Bergeman CS (2019) On standardizing within-person effects: potential problems of global standardization. *Multivar Behav Res* 54:382–403. <https://doi.org/10.1080/00273171.2018.1532280>
- Watanabe T, Saito K, Ishida K, Tanabe S, Nojima I (2018) Age-related declines in the ability to modulate common input to bilateral and unilateral plantar flexors during forward postural lean. *Front Hum Neurosci* 12:254. <https://doi.org/10.3389/fnhum.2018.00254>
- Winter DA (2009) *Biomechanics and motor control of human movement*. John Wiley & Sons, New Jersey
- Yamagata M, Falaki A, Latash ML (2018) Stability of vertical posture explored with unexpected mechanical perturbations: synergy indices and motor equivalence. *Exp Brain Res* 236:1501–1517. <https://doi.org/10.1007/s00221-018-5239-x>
- Yamagata M, Popow M, Latash ML (2019) Beyond rambling and trembling: effects of visual feedback on slow postural drift. *Exp Brain Res* 237:865–871. <https://doi.org/10.1007/s00221-019-05470-w>
- Yoshihara H, Hasegawa K, Okamoto M, Hatsushikano S, Watanabe K (2018) Relationship between sagittal radiographic parameters and disability in patients with spinal disease using 3D standing analysis. *Orthop Traumatol Surg Res* 104:1017–1023. <https://doi.org/10.1016/j.otsr.2018.07.009>
- Zhang L, Feldman AG, Levin MF (2018) Vestibular and corticospinal control of human body orientation in the gravitational field. *J Neurophysiol* 120:3026–3041. <https://doi.org/10.1152/jn.00483.2018>

Publisher's Note Springer Nature remains neutral with regard to jurisdictional claims in published maps and institutional affiliations.